Consistent size dependency of core-level binding energy shifts and single-electron tunneling effects in supported gold nanoclusters

Taizo Ohgi* and Daisuke Fujita
National institute for Materials Science, 1-2-1 Sengen, Tsukuba, Ibaraki, 305-0047, Japan
(Received 8 March 2002; revised manuscript received 28 May 2002; published 19 September 2002)

Uniform Au-clusters supported on well-defined substrate [octanedithiol/Au(111)] were analyzed by tunneling and x-ray photoelectron spectroscopy. Single-electron tunneling effect and the binding-energy shift observed in these spectroscopies exhibit the consistent cluster-size dependency. Au $4f$ core-level shift of the supported clusters can be well explained by the charging energy $e^2/2C$, where C is the capacitance between a cluster and its surroundings. The main contributions to this C are the self-capacitance of the cluster, the dielectric constant of the octanedithiol layer ($\epsilon \sim 3$) and the effect of the substrate. The other possible contributions are attributed to the effect of nearest-neighbor clusters and the electron spillout from the cluster and substrate due to the coupling between the molecular orbital and the conducting electrons.

DOI: 10.1103/PhysRevB.66.115410 PACS number(s): 73.22.−f, 79.60.−i, 73.23.Hk

I. INTRODUCTION

The ionization potential I and the electron affinity A of small metal clusters with a variety of diameters mediate between those of an atom and the work function W of a bulk solid [Fig. 1(a)].[1] The main origin of the difference of A and I from W is the classical electrostatic effect to inject an electron or a hole in the limited space. When a cluster with a radius of R exists in a vacuum, the self-capacitance (the capacitance toward grounded infinity) is defined as $C_{\mathrm{self}} = 4\pi\epsilon_0 R$ from the simple conducting-sphere model. For electron injection and extraction in a small cluster system, the charging energy $e^2/2C$ of a cluster should be taken into account. In a classical model, A and I for the cluster can be expressed by

$$A = W - e^2/2C = W - \mu(1),$$
$$I = W + e^2/2C = W - \mu(0), \tag{1}$$

where $\mu(N)$ is the chemical potential of the cluster when the number of excess electrons changes from $N-1$ to N. It is obvious that A and I depend on the cluster size and converge on W in the infinite limit, which has been intensively studied by photoionization and photoelectron spectroscopy with free cluster beams[1] or supported clusters.[2,3]

On the other hand, tunneling spectroscopy can also measure the chemical potential of a cluster through the single-electron tunneling (SET) effect.[4] When a cluster is placed between two electrodes with the distance at which tunneling of electrons is possible, the current can flow only when the Fermi energy of the electrode exceeds the chemical potential of the cluster (Coulomb blockade) as shown in Fig. 1(b). When the number of excess electrons in the cluster changes from N to $N+1$, the chemical potential $\mu(N+1)$ is given by $(2N+1)e^2/2C_{\mathrm{total}}$, where C_{total} is the total capacitance of the cluster towards the environment including electrodes. When the two tunnel junctions have appropriate structures, the current changes stepwise as the excess electrons increase one by one (Coulomb staircase). The main interest for SET devices is to fabricate a structure as small as possible, so that the charging energy of the system $e^2/2C_{\mathrm{total}}$ can overcome the electron thermal energy $k_B T$. The lower limit of the total capacitance of a center island is its self-capacitance C_{self}, and hence, the upper limit of the charging energy is $e^2/2C_{\mathrm{self}}$. In the case of a cluster with a diameter of 1 nm, C_{self} is $\sim 10^{-19}$ F and $e^2/2k_B C_{\mathrm{self}} \sim 10^4$ K, which allows the device operation at room temperature.[5,6]

In this paper, we report that the binding-energy shift of the supported metal clusters has the origin in their chemical potential $\mu(0)$ determined by the capacitance between the cluster and the substrate [Fig. 1(c)]. Gold deposited octanedithiol/Au(111) samples provide uniformly sized Au nanoclusters [Fig. 1(d)], well-defined tunneling barriers and atomically flat substrate,[7] which enables us to compare ex-

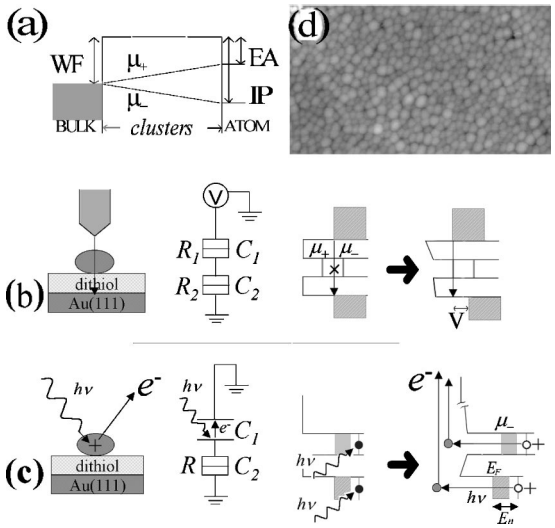

FIG. 1. (a) Work function of a bulk metal, and ionization potential (IP) and electron affinity (EA) of an atom. IP and EA of clusters mediate between them. μ_+ and μ_- denote the chemical potentials $\mu(1)$ and $\mu(0)$, respectively; (b) Schematic diagram and equivalent circuit for tunneling spectroscopy on Au-cluster/octanedithiol/Au(111) sample; (c) Those for photoelectron spectroscopy; and (d) STM image of Au-nanoclusters grown on octanedithiol/Au(111) substrate at 1.9 monolayer coverage (104 nm×60 nm).

perimental results with simple physical models and also minimizes the fluctuation of macroscopic data obtained by photoelectron spectroscopy. Scanning tunneling microscopy and tunneling spectroscopy can clarify the coupling amplitude of a cluster with the substrate geometrically and electrically. Spectroscopy at low-temperature provides the coupling parameters of each cluster, most of which were not able to be determined in the measurements at room temperature due to the thermal fluctuation.[7] We examined the prepared samples by photoelectron and tunneling electron spectroscopies independently and found that the results from both spectroscopies show consistent cluster-size dependence in the charging effect of supported metal clusters.

II. EXPERIMENTAL

The preparation method of the samples was reported elsewhere.[7] The size of the clusters can be controlled by the amount of Au deposition on octanedithiol/Au(111) substrate. These nanoclusters, 10–30 Å in diameter with small standard deviation (σ, less than 15% of the diameter), spread over the surface with a density of $1.2–0.6\times10^{13}/\mathrm{cm}^2$ for Au-apparent coverage between 0.25–4 monolayers (ML) [Fig. 1(d)]. The octanedithiol layer on Au(111) is homogeneous and has $\sim$10 Å in thickness.

Tunneling spectroscopy was performed by using a variable-temperature scanning tunneling microscope (VT-STM, Omicron) in UHV ($\sim10^{-8}$ Pa) at the temperature of $\sim$30 K. In order to minimize the effect of the work-function difference, Au-coated tungsten tips (1000 Å in thickness deposited by dc-Magnetron sputtering) were used. The spectroscopy was performed under high set-impedance conditions ($R>10$ GΩ). The radius of clusters was determined from the density of clusters and the amount of Au-deposition assuming the spherical shape of the clusters. The parameters [the resistance and capacitance between a tip and a cluster (R_1,C_1), ones between a cluster and a substrate (R_2,C_2) and residual charge (Q_0), see Fig. 1(b)] were obtained by least squares fittings of $I-V$ curves (Coulomb staircase) using the orthodox theory[8] with barrier suppression modification.[9] To determine these parameters for a cluster, the fittings were separately performed for more than ten $I-V$ curves obtained by single bias sweep (i.e., not averaged) and the dispersions of each parameter were checked.

X-ray photoelectron spectroscopy (XPS, PHI 5400) with Mg-$K\alpha$ x-ray (1253.6 eV and 200 W) and a pass energy of 35.75 eV was used for the observation of Au $4f$ core-level spectra. To enhance the cluster contribution to the spectra, a shallow takeoff angle (15°) of photoelectrons was selected. The cluster contribution to each Au $4f$ spectrum was obtained by subtracting the spectrum obtained on octanedithiol/Au(111) substrate, with the amplitude determined by the attenuation of the C $1s$ spectrum from octanedithiol layer.

III. RESULTS AND DISCUSSION

Due to the small self-capacitance of these clusters, it is possible to observe Coulomb blockade even at room temperature.[5,7] However, Coulomb staircase is infrequently

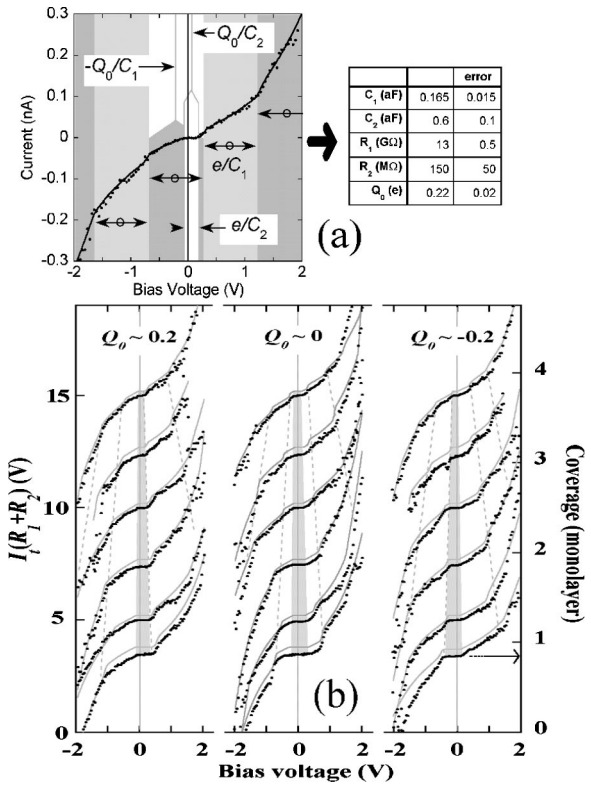

FIG. 2. Typical $I-V$ curves obtained by single bias sweep at $\sim$30 K. Solid curves are results of curve fittings by the orthodox theory with barrier suppression.[9] (a) Coulomb staircase from a cluster formed after 2.5 ML Au coverage and obtained parameters. (b) The curves with Q_0 of $\pm0.2e$ and 0 are put together with the offsets proportional to the Au coverage (right axis).

observed since the double tunnel junctions in our system are under the conditions, $C_1/C_2<1$ and $R_1/R_2>1$, which makes the characteristics on $I-V$ curves smaller[10] and the thermal energy smears these fine structures. Although the measurement at room-temperature provided the qualitative analysis of the cluster-size dependency in the charging effect through the gaps in $I-V$ curves,[7] the quantitative evaluation of this system have been needed to compare the microscopic and macroscopic results from two spectroscopies in detail. The observation at low temperature can clarify the thermally smeared features in $I-V$ curves and hence, the physical parameters around each cluster. Typical $I-V$ curves are shown in Fig. 2. The classification in Ref. 10 reveals that all curves obtained in our experiments belong to either case I ($Q_0>0$), II ($Q_0\sim0$) or IV ($Q_0<0$) and do not belong to case III [$C_1/C_2, R_1/R_2>1(<1)$] without exception. As seen in Fig. 2(a) the center gaps around the origin depend on C_2 and Q_0 as $(Q_0-e/2)/C_2<V<(Q_0+e/2)/C_2$, while the periodic structures in the curves depend on C_1 and Q_0 as $(ne-Q_0-e/2)/C_1$, where $n=0,\pm1\ldots$.[4] These large periodic structures minimize the fluctuation of C_1 and Q_0 during curve fittings, resulting in smaller errors (less than 10%). It is obvious that the capacitance C_1 and C_2 are strongly dependent on the cluster size as seen in Figs. 2(b) and 3(a); with increasing cluster size C_1 and C_2 increase monotonically. The capacitances of each sample were determined from more

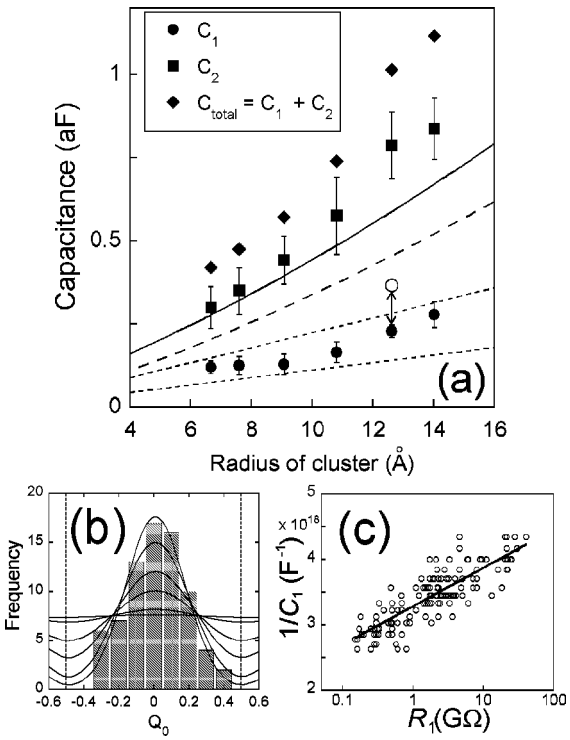

FIG. 3. (a) Cluster-size dependence of the capacitances C_1, C_2, and C_{total}. Each point is obtained from more than ten clusters randomly selected and the bars show the standard deviations. The dotted lines denote the self-capacitance of a free cluster (lower) and one supported on the layer ($\epsilon \sim 3$), respectively. The dashed curve denotes the capacitance including the contribution from the tip and substrate. The solid curve also includes the effect of sulfur atoms causing the electron spillout from the cluster and substrate (see text). Arrows and an open circle indicate the variation of C_1 shown in (c). (b) Distribution of Q_0 obtained in this study. Solid curves denote Gaussian distributions assuming the periodic feature of Q_0, which have σ of $0.17e$, $0.2e$, $0.25e$, $0.3e$, $0.4e$, and $0.5e$ from the top at $Q_0=0$, respectively. (c) Relation between R_1 and C_1 taken for one cluster grown after 3 ML deposition ($R \sim 12.5$ Å).

than ten clusters randomly selected. The standard deviations [bars in Fig. 3(a)] are 10–20 % of these values, in good agreement with those of the cluster size[7] since the self-capacitance, main contribution to the total capacitance, should be proportional to the cluster size.

Coulomb staircase curves provide the information about the chemical potential differences between electrodes and a cluster. It was found that each cluster has its specific value for Q_0 and these values for the whole observed clusters distribute around $Q_0 \sim 0$ as shown in Fig. 3(b) ($\overline{Q_0}=0.01e$ and $\sigma=0.17e$). This clearly shows that $[\mu(1)+\mu(0)]/2$ of the clusters is nearly equal to the Fermi level of the tip and substrate at zero bias. As shown in the figure, Gaussian distribution, in which the periodic feature of Q_0 is taken into account, well-describes obtained results. More than 99% of clusters have $|Q_0|$ of less than 0.5 when $\sigma=0.17e$ and even in a worse case ($\sigma=0.3e$), more than 90% of clusters are in this range, indicating that most of clusters on substrate are electrically neutral.

All the obtained $I-V$ curves can be fitted by the orthodox theory. However, in the small structure that has a small center island with the same size of tunneling barriers, the main contribution to the total capacitance of the cluster towards surroundings is the self-capacitance of the cluster, while the contribution from the electrodes is less than ~30% of the total capacitance.[11] When the cluster is not charged (i.e., neutral), the electric-field applied by electrodes polarizes the cluster and accumulated charges ($\pm Q'$) appear on both the sides of the cluster surface. Although the capacitances determined by $C'_{1(2)}=Q'/V_{1(2)}$, where $V_{1(2)}$ is the voltage drop at the gap 1(2), could be small enough when the gap has longer distances, $C'_1+C'_2$ can not give the total capacitance and apparently, $C'_{1(2)}$ is not equal to $C_{1(2)}$ obtained by above curve fittings since $C'_{1(2)}$ ignores the self-capacitance contribution of the cluster. It is necessary, therefore, to check the applicability of simple curve fittings of double tunneling junctions to this system. In order to include the self-capacitance contribution, we introduce the gate capacitance (which is equal to C_{self}) with the gate voltage that is automatically set to the electric potential of the center island without excess charge [$V_G=C'_1V/(C'_1+C'_2)$ in the circuit of Fig. 1(b)]. In this system the total capacitance C_{total} is $C'_1+C'_2+C_{\text{self}}$ and this circuit acts like the double tunneling junctions without gate whose capacitances are described by $C_{1(2)}=C_{\text{total}}C'_{1(2)}/(C'_1+C'_2)$. These capacitances satisfy $C_1+C_2=C_{\text{total}}$ and $C_1/C_2=C'_1/C'_2$, which indicates that the orthodox theory for the double tunneling junctions can be applicable in this system without modification although the self-capacitance does not explicitly appear, and hence, C'_1 and C'_2 are unknown from the curve fittings.

In order to investigate the tunneling barrier 1, the relation between R_1 and C_1 was studied as shown in Fig. 3(c). The parameters were obtained for one cluster with the constant bias voltage of 1 V and the set currents varied from 50 pA to 5 nA. In a simple model, R_1 and C_1 can be roughly expressed by, $R_1=R_0\exp(\lambda d)$ and $C_1=A/d$, where λ is $1.025\sqrt{\phi}$ (ϕ is the work function in eV) and d is the distance between the tip and the cluster. By the curve fitting and taking the typical value for λ (~2.2), it can be determined that $R_0=2.6$ KΩ and $A=1.8$ aF Å. When $R_1=10$ GΩ, the tip-cluster distance d is estimated to be about 7 Å. This indicates that the clusters exist nearly at the middle between the tip and Au(111) surface. Since the curvature of the tip apex is much larger than that of the clusters, the approximation of a cluster existing inbetween two flat plates is valid and therefore, the ratio between C_1 and C_2 ($C_2/C_1 \sim 3$) as seen in the figure can be attributed to the dielectric constant of octanedithiol layer[12] ($\epsilon \sim 2.7$) which exists only between the clusters and Au(111) substrate. Although the above relation between C_2 and C'_1 indicates that C_2 depends on the tip position, $C'_1 \ll C'_2$ due to high-ϵ minimizes this dependency.

The total capacitance of the cluster can be numerically calculated as shown in Fig. 3(a). Even after the consideration about the self-capacitance, the effect of the tip and substrate, and dielectric constant of the dithiol layer, the calculated one (dashed curve in the figure) is not enough to explain the obtained C_{total} ($=C_1+C_2$). The possible origin will be discussed later.

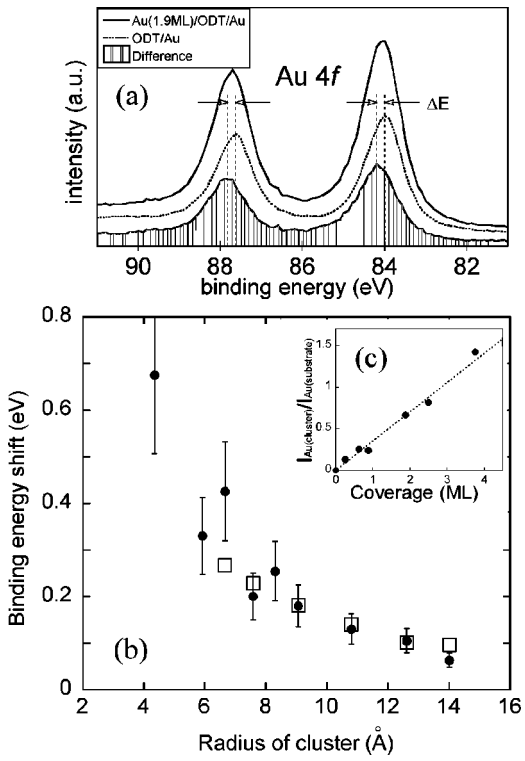

FIG. 4. (a) Au $4f$ spectra from octanedithiol/Au(111) substrate and Au (1.9 ML) deposited one. The shaded area is the difference between these spectra. (b) Cluster-size dependence of Au $4f$ core-level shift. Open squares are charging energy derived from the results of tunneling spectroscopy ($e^2/2C_2$). (c) Coverage dependence of the ratio between cluster and substrate components in the Au $4f$ spectra.

The binding energy of Au $4f$ core-level from the clusters also exhibits the cluster-size dependence as shown in Fig. 4. The shallow takeoff angle (15°) of the photoelectrons enhances the contribution of the clusters whose growth is proportional to the coverage [Fig. 4(c)]. Comparing with the photoelectron from bulk metal, the emitted photoelectron from a cluster feels positive charge left in the cluster. This hole will be filled by the electron supplied from the substrate, but it takes about $t=R_2C_2\sim 100$ psec typically, long enough to lower the kinetic energy of the emitted electron but short enough to keep most of the clusters electrically neutral. Thus as shown in Fig. 1(c), the difference of the kinetic energy E_K can be expressed by

$$E_{K,\mathrm{cluster}}=h\nu-E_n-\Phi+\mu(0)=E_{K,\mathrm{bulk}}+\mu(0), \qquad (2)$$

where $h\nu$ is the energy of photon, E_n is the binding energy of atomic core level and Φ is the work function of the spectrometer. With respect to the bulk binding energy, the spectral peaks move higher with decreasing cluster size. It is obvious that the binding-energy shift and the charging energy derived from $e^2/2C_2$ show consistent cluster-size dependency qualitatively and quantitatively. The capacitance between substrate and clusters determines the chemical potential of cluster $\mu(0)$, leading to the core-level binding-energy shift.

Full width at half maximum of the spectra from bulk Au is 1.1 eV, while one from clusters is ~1.2 eV. This origin can be ascribed to following aspects. (i) The deviation of the cluster size and the barrier thickness, which directly leads to the deviation of C_2 (~15%), and hence, the charging energy (~0.1 eV). (ii) The deviation of $Q_0(\pm 0.2e)$ leads to the deviation of charging energy, 0.1~0.2 eV. The lifetime of the ionized states of clusters could affect the linewidth.[13] However, as estimated above, the lifetime of the state ($R_2C_2\sim 100$ psec) is too long to affect the linewidth.

Although the charging effects independently obtained from both tunneling and photoelectron spectroscopies show consistent size dependency, the absolute value of C_{total} is not explained enough by the simple model. One, which can explain this discrepancy, is that the effective cluster size could be larger than the calculated one. The Au(111) substrate and clusters are covered with terminal sulfur atoms of octanedithiol molecules. The dithiol molecules have highest occupied and lowest unoccupied molecular orbitals around sulfur atoms that is chemically bound to Au atoms. These molecular orbitals are hybridized with the conducting electrons in the clusters and the Au(111) surface, which could make the effective tunneling distance between the cluster and the Au(111) substrate smaller and the effective-cluster-size larger, and hence, C_2 larger. Even if the increase of the density of states due to the coupling is not existing at the Fermi level, SET effect occurs at higher bias voltages (>0.5 V) in our system and therefore, coupling states cannot be negligible. Actually, the observation of the self-assembled monolayers of thiol molecules by STM shows that sulfur atoms in the molecules contribute the topographic images as if they were metallic adatoms (~1.8 Å in apparent height),[14] and also the thickness of the dithiol layer contributes the height profile of the clusters in STM images.[7] If this effect is taken into account, the barrier width is reduced by ~3.6 Å and the effective cluster radius increases by ~1 Å, enhancing the total capacitance as shown in the figure (solid curve). Another possible explanation for this discrepancy is the effect of the nearest-neighbor clusters. The charging-up of the cluster causes the charge polarization of the neighbor clusters, leading to the increase of C_2. This effect becomes unnegligible above the Au coverage of 2.5 ML ($R>10$ Å).

It has been reported for free clusters theoretically and experimentally that the electron spillout and other quantum-mechanical effects change classical $1/R$ dependence of the ionization potential and the electron affinity shown in a Eq. (1).[1,15] In the case that the self-capacitance is dominant in the total capacitance of supported clusters, there is no reason that the capacitances are independent on the number of excess electrons. These effects would cause strong asymmetric features in $I-V$ curves and the orthodox theory for SET would need modifications. However, in this study the simple model can be applied even to the smallest clusters (~100 atoms) that have large periodic features on $I-V$ curves with $\overline{Q_0}$ of ~0, implying that the chemical potentials of the cluster $\mu(N)$ are equally spaced and symmetrical against the Fermi energy of the substrate. Much smaller clusters might be needed for the considerations of these effects.

Although the above discussions in the core-level binding-

energy shifts are based on the final-state effect, other influences originated from the initial-state effects might be important. The effect of the chemical potential difference between clusters and substrate should be ruled out as discussed in Q_0 distribution, but only affects the linewidth. It is well known that the electronic states of atoms on the topmost surface are different from those of underlayer atoms, leading to the surface-atom core-level binding-energy shifts.[16] For a nanocluster with the diameter of ~ 10 Å, more than 70% of total atoms appear on the cluster surface. It has reported that bulk gold has a significant negative surface core-level shift (~ 0.4 eV),[16] which would be large enough to cancel out the positive shifts coming from the charging effects. However, our results have exhibited the close agreement between the core-level binding-energy shifts and the charging energy $e^2/2C_2$ derived from the tunneling spectroscopy over a wide range of cluster size, indicating that the core-level shift is dominated by the final-state effect. This result is consistent with the formerly reported ones that the apparent Fermi level in clusters obtained from valence-band data exhibits the shifts close to the core-level binding-energy shift.[2,3] There is no reason that the atoms of cluster surface should have the same physical properties with those of bulk surface. However, these results do not mean that the initial-state effects are absent in this system since they might be canceled out with other effects. The initial-state effects should exist and have to be taken into account for a more complete analysis.

IV. SUMMARY

We studied uniform Au-clusters supported on octanedithiol/Au(111) substrate by tunneling spectroscopy and x-ray photoelectron spectroscopy. The absolute value of the chemical potentials of the clusters, $\mu(0)$ and $\mu(1)$, can be described by the $e^2/2C$, where C is the capacitance of the cluster against the environment. This capacitance includes the self-capacitance of the cluster, depending on the cluster size, and the capacitance between the cluster and the substrate covered by the octanedithiol layer. The latter one increases the total capacitance and hence, lowers the charging energy. Comparing with the free cluster system, the emitted electron feels the polarized charges appeared at the octanedithiol layer and the image negative charge accumulated on the Au(111) surface in addition to the hole left in the cluster. Although each cluster has the specific value of $[\mu(0)+\mu(1)]/2$, the mean value is nearly equal to the Fermi energy of the grounded Au(111) substrate, indicating that the ionization potential and the electron affinity are symmetrical against the work function of the bulk Au substrate. Although photoelectron spectroscopy only provides the information of the ionization potential, tunneling spectroscopy shows that of the electron affinity, and moreover that of the secondary and higher order ionization potentials and electron affinities.

ACKNOWLEDGMENTS

The authors would like to acknowledge M. Yoshitake for her support in XPS measurement, and Z.-C. Dong and H. Goto for helpful comments. This study was performed through Active Nano-Characterization and Technology Project, Special Coordination Funds of the Ministry of Education, Culture, Sports, Science and Technology of the Japanese Government.

*Electronic mail address: OHGI.Taizo@nims.go.jp

[1] W.A. de Heer, Rev. Mod. Phys. **65**, 611 (1993), and references therein.
[2] G.K. Wertheim, S.B. DiCenzo, and S.E. Youngquist, Phys. Rev. Lett. **51**, 2310 (1983).
[3] G.K. Wertheim, S.B. DiCenzo, and D.N.E. Buchanan, Phys. Rev. B **33**, 5384 (1986).
[4] M. H. Devoret and H. Grabert, in *Single Charge Tunneling*, Vol. 294 of NATO Advanced Studies Institute, Series B: Physics, edited by H. Grabert and M. H. Devoret (Plenum, New York, 1992).
[5] D. Anselmetti, T. Richmond, A. Baratoff, G. Borer, M. Dreier, M. Bernasconi, and H.-J. Güntherodt, Europhys. Lett. **25**, 297 (1994).
[6] K. Matsumoto, M. Ishii, K. Segawa, Y. Oka, B.J. Vartanian, and J.S. Harris, Appl. Phys. Lett. **68**, 34 (1996).
[7] T. Ohgi, H.-Y. Sheng, Z.-C. Dong, H. Nejoh, and D. Fujita, Appl. Phys. Lett. **79**, 2453 (2001).
[8] M. Amman, R. Wilkins, E. Ben-Jacob, P.D. Maker, and R.C. Jaklevic, Phys. Rev. B **43**, 1146 (1991).
[9] A.N. Korotkov and Y.V. Nazarov, Physica B **173**, 217 (1991).
[10] A.E. Hanna and M. Tinkham, Phys. Rev. B **44**, 5919 (1991).
[11] M. Macucci, K. Hess, and G.J. Iafrate, Phys. Rev. B **48**, 17354 (1993).
[12] M.A. Rampi, O.J.A. Schueller, and G.M. Whitesides, Appl. Phys. Lett. **72**, 1781 (1998).
[13] H. Hövel, B. Grimm, M. Pollmann, and B. Reihl, Phys. Rev. Lett. **81**, 4608 (1998).
[14] G.E. Poirier and E.D. Pylant, Science **272**, 1145 (1996).
[15] M. Seidl, K.-H. Meiwes-Broer, and M. Brack, J. Chem. Phys. **95**, 1295 (1991).
[16] P.H. Citrin, G.K. Wertheim, and Y. Baer, Phys. Rev. B **27**, 3160 (1983).